

## Semi-rigidity of cap plate and extended end plate connections

Dia Eddin Nassani<sup>\*1</sup>, Abdul Hakim Chikho<sup>2a</sup> and Aliriza İlker Akgönen<sup>3b</sup>

<sup>1</sup>Department of Civil Engineering, Hasan Kalyoncu University, Havalimani yolu 27410, Gaziantep, Turkey

<sup>2</sup>Faulty of Civil Engineering, Aleppo University, Aleppo, Syria

<sup>3</sup>Department of Civil Engineering, Kahramanmaraş Sutcu Imam University, Kahramanmaraş, Turkey

(Received August 12, 2016, Revised January 14, 2017, Accepted January 20, 2017)

**Abstract.** The behaviour of steel frames is highly influenced by the beam-column connections. Traditionally, Steel frames were usually designed assuming that connections are ideally pinned or fully rigid. A semi-rigid connection, however, creates a balance between the two extreme approaches mentioned above. In this research, two full scales of Extended End Plate Connections (EEPCs) were tested. Mathematical and numerical models were used to analyse the connections, and close correlations were found between these models and the corresponding tested specimens, which confirmed the confidence in the experimental results. The experimental results obtained enrich the available test data about behaviour of EEPC. In addition, the purpose of studying EEPC experimentally is to compare the stiffness and moment-rotation curve of EEPCs with that of Cap Plate Connections (CPCs), which were tested in a previous work. CPCs have not been studied sufficiently in the literature. The results obtained show that the typical CPC reduces the connection stiffness and these results will make a valuable contribution to the available test data in the research area of CPC.

**Keywords:** extended end plate; cap plate; semi-rigid connection; experimental test; moment-rotation curve

### 1. Introduction

In the analysis and design, connections are characterized as either fully rigid or ideally pinned. A semi-rigid connection creates a balance between the two extreme approaches mentioned above. This classification is characterized by the nonlinear moment-rotation relationship, which must be incorporated in the analysis (Del Savio et al. 2009). Studies agree that in analysis of frames, the connection rotational behaviour must be well-considered (Lui and Chen 1987, Jaspert and Maquoi 1990, Faella et al. 2000). Eurocode 3 (2005) classifies the connections in terms of stiffness and strength. Considering the stiffness, a connection is considered as pinned, semi-rigid, or rigid through the value of  $EI/L$ , where 'E' stands for the elasticity modulus, 'I' stands for the moment of inertia, and 'L' stands for the length of the connected member. If the initial rotational stiffness is less than  $0.5EI/L$ , the connection is classified as pinned connection, while it is rigid if the initial rotational stiffness is greater than  $25EI/L$ . The semi-rigid connection falls between these two boundaries. Considering the connection strength, a connection is classified as nominally pinned, partial-strength, or full-strength through comparisons with the design plastic moment resistance of the connected member.

In the Allowable Stress Design specification (AISC

ASD 1989), frame structures are divided into three basic categories. First is rigid frame that assumes beam-to-column connections have sufficient rigidity to hold the original angles between the intersecting members virtually unchanged. The second is simple frame that the ends of beams are connected for shear only and are free to rotate under loads. The third category is semi-rigid framing, where the connections of beams possess a dependable and known moment capacity that is intermediate in degree between the rigid and simple framing. In the Load and Resistance Factor Design specification (AISC LRFD 2005), only two categories define the types of frame structures. One is fully-restrained in which beam-to-column connections have sufficient rigidity to hold the original angles between intersecting members virtually unchanged. The other is partially-restrained in which the connections of beams and girders possess a sufficient rigidity between the intersecting members.

Baniotopoulo and Wald (2000) classified the connection regarding stiffness into rigid joints, pinned joints and semi-rigid joints. Regarding the strength classification, it consists simply in comparing the connection moment resistance with two reference resistances that are given by so-called full strength boundary and pinned boundary. The pinned boundary corresponds to 25% of the full-strength boundary. The connection is said full-strength, when its resistance exceeds the full-strength boundary, pinned, when it is lower than the pinned boundary, and partial-strength, when it lies between these two boundaries.

According to Salmon et al. (2009), the typical rigid connection would have to carry an end moment about 90% or more. The simple connection may have to resist only 20% or less of moment, while the semi-rigid connection

\*Corresponding author, Assistant Professor,  
E-mail: [diaeddin.nassani@hku.edu.tr](mailto:diaeddin.nassani@hku.edu.tr)

<sup>a</sup> Professor, E-mail: [ahchikho@hotmail.com](mailto:ahchikho@hotmail.com)

<sup>b</sup> Assistant Professor, E-mail: [ilkerakgonen@ksu.edu.tr](mailto:ilkerakgonen@ksu.edu.tr)

would be expected to resist some intermediate value at about 50% of the fixed end moment. Jaspert *et al.* (1999) developed a numerical approach aiming to analyse the connection behaviour from the first loading steps up to collapse, the connection subjected to bending moment and axial force. This approach is idealised by a mechanical model comprising extensional springs. Each spring represents a joint component by exhibiting non-linear force-displacement behaviour.

The extended end-plate connection has a high stiffness characteristic, which is often designed to develop the full moment capacity of jointing beams before connection fails. Many publications have mentioned that EEPC is a typical rigid connection (Bai *et al.* 2015, Coelho *et al.* 2004). A schematic comparison for the connection behaviour of different types of connections is illustrated in Fig. 1 and shows that EEPC has a moment capacity about 90% (Hayalioglu and Degertekin 2005). Tahir *et al.* (2008) tested two full-scale connections, one with flush end-plate and the other with extended end-plate connections. It was concluded that, the use of extended end-plate connections has significant increase in the moment resistance compared with flush end-plate connection.

The use of semi-rigid connections is very common among researchers due to its advantages (Patnana and Vyavahare 2016, Al-Jabri *et al.* 2005, Thai *et al.* 2016). The advantage of a design utilizing a semi-rigid connection over rigid connection is that beam-moments and column-

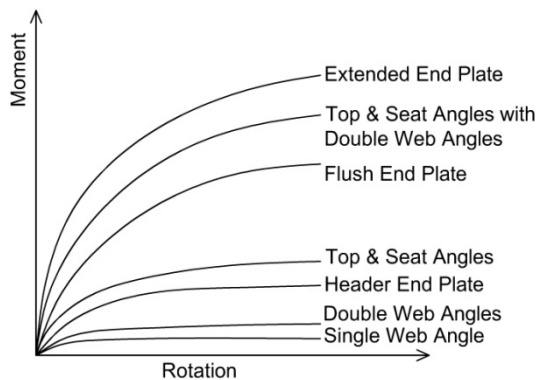


Fig. 1 Comparison of Moment-Rotation relation for different connections (Hayalioglu and Degertekin 2005)

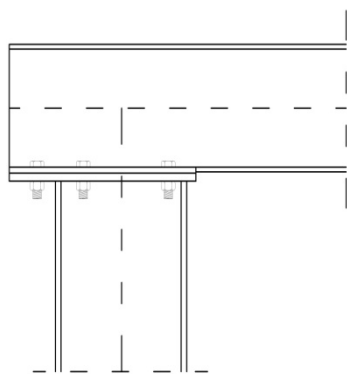


Fig. 2 Cap plate connection

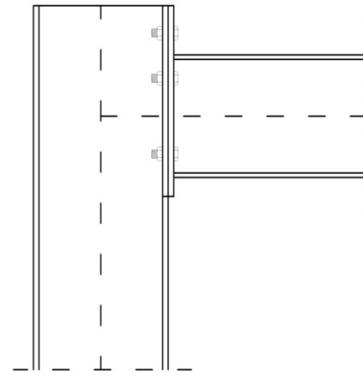


Fig. 3 Extended end plate connection

moments are reduced leading to lighter elements in many cases (Bose and Hughes 1995, Jones *et al.* 1983). The benefits of cost saving of multi-storey steel frames using semi-rigid connections have been proven to be more than simple connections (Couchman 1997). It was mentioned that the savings in steel weight of using semi-rigid connection alone in multi-storey braced steel frames using British hot-rolled section was up to 12% (Weynand *et al.* 1998).

Of the various types of beam-column connections used in industrial frames, single or multiple bays, CPC shown in Fig. 2 is frequently used. It has many important advantages over EEPC shown in Fig. 3. CPC is easier to erect and more economical (El-Boghdadi 1998, Nassani 2011). In CPC, only the bottom flange of the beam is connected to the column. This invariably introduces greater flexibility at the joint than EEPC, in which the beam is connected to the side of the column. CPC is a typical case of a semi-rigid connection, which allows an appreciable amount of rotation even at the service level (El-Boghdadi 1998).

El-Boghdadi (1998) studied six full scale cap plate connections and concluded that the use of vertical web stiffeners in beams at the connection increases the connection stiffness. The normal strains are approximately null at the upper flange near the corner due to the path of the moment from the beam to the column, which is dependent on the bolts and the plates in contact between the beam and the column.

According to Nassani (2014), the thickness of the beam bottom flange plate at the connection location influences both the initial rotation stiffness and the ultimate moment capacity of the cap plate connection, which increases with the increase of plate thickness by preventing high plate deformation. The web thickness of the beam at the connection location affects the initial stiffness and the ultimate moment due to shear deformation in the web panel. The initial stiffness decreases with thinner webs due to increased shear deformation.

In this research, two full scale of EEPCs have been tested. The main purpose of studying EEPC experimentally is to compare the stiffness and moment-rotation curve of EEPCs, which is considered rigid connection in many literatures (Bai *et al.* 2015, Coelho *et al.* 2004, Scerbo 1996), with that of CPCs which were tested in a previous work (Nassani 2014). The researchers investigated the

rigidity of EECC and CPC. The column and beam cross-section, beam plate (PL1), column plate (PL2), bolts diameter, and weld thickness are the same for the compared specimens.

## 2. Methodology of research

### 2.1 Test specimens and techniques

The test specimen selected in this experimental is a cantilever sub assemblage of a beam and column, representing a portion of moment-resisting frame (Bose and Hughes 1995). The typical cantilevered beam specimen used is shown in Fig. 4. The size of the flange plates and web plates for the beam and column for each test is shown in Table 1.

In this research, two full scales of EEPs have been tested and compared with experimental results of CPCs tested in a previous work (Nassani 2014). The EEPs specimens have the same beam and column section, bolt diameter, and weld thickness of that of CPCs. The comparison is based on the moment-rotation curves of each connection type. The moment-rotation relationship is recorded using the traditional cantilever test setup (Bose and Hughes 1995).

The rotation of the joint was monitored using four LVDTs connected to a data acquisition system; LVDTs were used to measure the displacements at several locations on the beam column connection. Locations of LVDTs were



Fig. 5 LVDTs locations

indicated in Fig. 5. The rotation of the connection was calculated by dividing the measured displacement for each LVDT by the distance between the LVDT and connection center (Fang *et al.* 2014, Penar 2005, El-Boghdadi 1998). Then the average of four rotations has been considered to plot the moment-rotation curve due to LVDTs. The moment applied to the connection was calculated by multiplying the force recorded by the hydraulic actuator with the distance from the actuator center to the column face (Abolmaali *et al.* 2009).

### 2.2 Materials properties

To determine the material properties, tensile test has been carried out on specimens taken from beam, column, and plates. A specimen of length 25 cm, width 3 cm, and collars at the ends is fitted in the grips of a testing machine. A gradually and slowly increasing tensile load  $P$  is applied on the sample through a mechanism provided in the machine. Due to the increasing tensile load, the specimen is continuously stretched. Stress and strain in the specimen are continuously recorded by the operator. The material properties, which are obtained from the test, are shown in Table 2. The bolts used for connecting the beam with the column are high strength bolts M 8.8.

### 2.3 Test procedure

The column was mounted first on the support system. Then column was supported by inclined double angle bracing to minimize bending deformation in the column. The beam was lifted and adjusted to the column. Then, the connection bolts were installed. The free end of the beam was laterally supported to prevent any lateral movement of the beam tip (cantilever end). The detail of the experimental set up has been described elsewhere (El-Boghdadi 1998 and Nassani 2014).

A small load was applied as a check and records were

Table 1 Specimens description (dimensions in mm)

Test No.	Column			Beam			Bolt Diam.
	Plate PL2	Web	Flange	Plate PL1	Web	Flange	
C1 Extended end plate	200 ×16	300 ×8	200 ×12	200 ×12	250 ×8	160 ×12	16
C2 Extended end plate	200 ×20	300×8	200 ×12	200 ×20	250 ×8	160 ×12	22

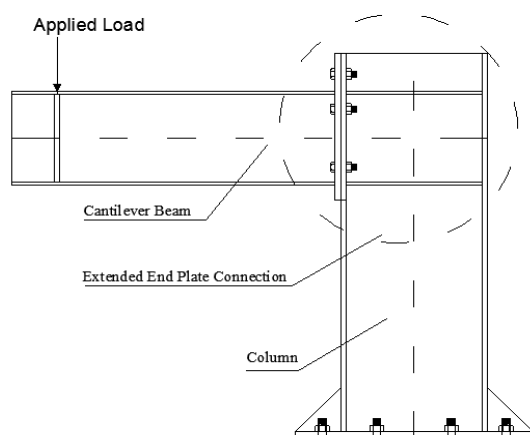


Fig. 4 Cantilever beam specimen for EEPC

Table 2 Material properties of the specimens

Ultimate strength (MPa)	Yield strength (MPa)	Modulus of elasticity (MPa)	Elongation at maximum load [%]
386	251	194063	15.77

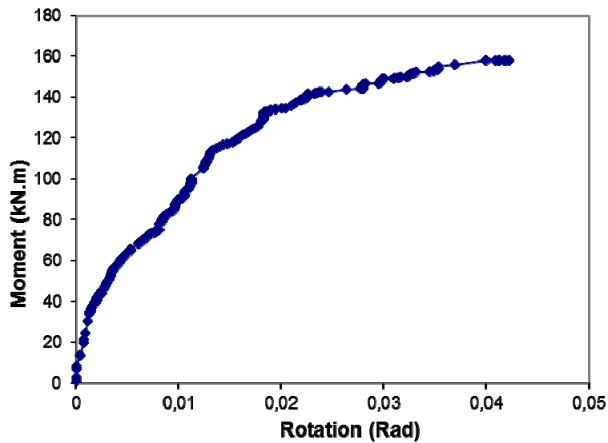


Fig. 6 Moment-Rotation relationship for specimen C1



Fig. 7 Connection deformation for specimen C1

taken from all the LVDTs to ensure that they were functioning as required. A vertical load was applied monotonically to the beam tip by a 50 ton hydraulic actuator. The applied load was monitored by connecting the hydraulic actuator to a data logger to automatically record the applied load. The load was applied at a slow rate and was incremented in steps. At each step of loading, the readings from LVDTs were recorded using the data logger. The loading was stopped at the incipient of failure, as judiciously observed from the deformation of the beam and the connection with no increase in the applied load.

### 3. Results

#### 3.1 Specimen C1

The plot of moment-rotation relationship for the specimen C1 (EEPC) is shown in Fig. 6. This is approximately linear up to a moment level of 80 kN.m. Thereafter, the moment-rotation plot becomes nonlinear up to the maximum moment 158 kN.m. This non-linearity indicates degradation in the connection stiffness represented by the slope of the curve. The initial stiffness of the plot is 14950 kN·m/rad. The connection deformations were observed as shown in Fig. 7.

#### 3.2 Specimen C2

The plot of moment-rotation relationship for specimen

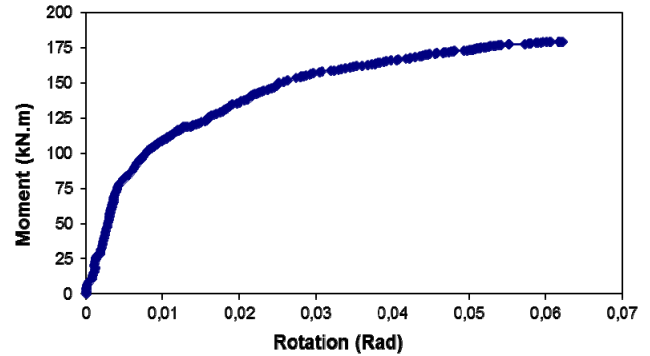


Fig. 8 Moment-Rotation relationship for specimen C2



Fig. 9 Connection deformation for specimen C2

C2 is shown in Fig. 8. This is approximately linear up to a moment level of 102 kN.m. Thereafter, the moment-rotation plot becomes nonlinear up to the maximum moment 179.5 kN.m. This non-linearity indicates degradation in the connection stiffness represented by the slope of the curve. The initial stiffness of the plot is 15400 kN·m/rad. The beam deflection was high at the end of the test as shown in Fig. 9.

## 4. Modelling of experimental specimens

### 4.1 Mathematical formulations

Different models were developed to express the nonlinear relationship between the applied moment and rotation for different types of connections. Three-parameter power model, proposed by Kishi and Chen (1990), was used to model the moment-rotation characteristics of the EEPC. It has the form

$$\theta_r = \frac{|M|}{R_{ki} \left( 1 - \left| \frac{M}{M_u} \right|^n \right)^{\frac{1}{n}}}$$

Where the three parameters are:

$R_{ki}$  is the initial stiffness of the connection,

$M_u$  is the ultimate moment capacity of the connection,

$n$  is a shape parameter.

Of the three parameters,  $R_{ki}$  and  $M_u$  must be calculated

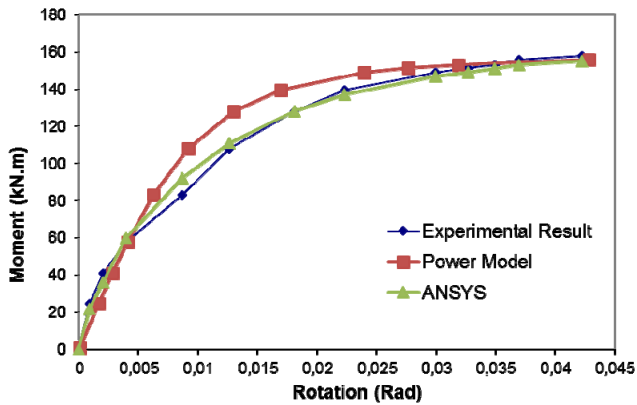


Fig. 10 Comparison between Power model, ANSYS and experimental test for specimen C1

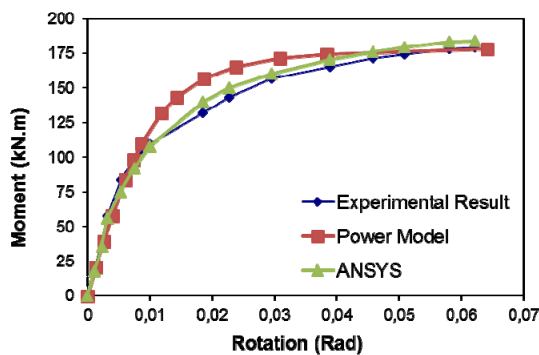


Fig. 11 Comparison between Power model, ANSYS and experimental test for specimen C2

for a connection as they would vary from connection to connection and the shape  $n$  controls essentially the shape of the moment rotation curve and its value can be established from the numerical adjustment to properly fit the experimental values.

#### 4.1.1 Comparison between Mathematical formulation and experimental values of $M-\phi$ :

(1) Specimen C1: Fig. 10 shows the plot of moment-rotation curves for power model and experimental result and close correlation were found between them, which confirm the confidence in the experimental results.

The parameters are:  $R_{ki}$  is equal to 14950 kN.m/rad (the initial slope of the curve as shown in Fig. 6),  $M_u$  is equal to 158 kN.m (the ultimate moment),  $n = 2.3$  (shape parameters).

(2) Specimen C2: The moment-rotation curves plotted in Fig. 11 show the comparison between the power model and the experimental result. The plot shows good correlation between the moment-rotation curves for power model and the experimental result.

The parameters are:  $R_{ki}$  is equal to 15400 kN.m/rad,  $M_u$  is equal to 179.5 kN.m,  $n = 2.2$ .

#### 4.2 Finite element analysis

To study the tested specimens, 3-D solid Finite Element

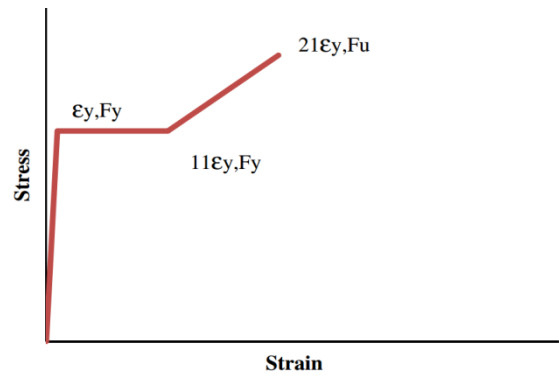


Fig. 12 Stress-strain curve for beam, column and cap plate material

(FE) models were developed. FE software ANSYS (2013) was used to create and analyze the specimen models. 8-node solid elements (SOLID185) have been used to model plates, beam, bolt heads, column and nuts. The bolt shank which connects the bolt head and nut was simulated using one 3-D spar element (LINK180). To model the pre-tension state in bolts, value of the initial stress was given to the spar element. The contact pairs were represented using 3-D Target (TARGE170) and Contact (CONTA174) elements to model the interface between beam plate and column cap.

All materials use Von-Mises yield criterion coupled with isotropic work hardening assumption. A tri-linear stress strain curve was used to describe the material properties (Bahaari and Sherbourne 1996). Fig. 12 shows the stress-strain curve which was used in the FE analysis to define the material property of beam, end plate and stiffeners. The stress-strain curve for high strength bolts is shown in Fig. 13.

ST37 steel was used to simulate the beam, column and plates, while M8.8 steel was used for the high-strength bolts. Boundary condition was defined as fixed support (Fixed Face).

The load was utilized in slow incremental rate to the beam tip. The slow rate of loading was applied to prevent the distortion of elements. Non-linear elastic plastic analysis has been performed, and the Newton-Raphson method (Ypma 1995) was used to solve the nonlinear equilibrium equations. The number of load substeps is equal to 5 and the convergence criterion is equal to 0.0005.

The plot of moment-rotation relationship using FE

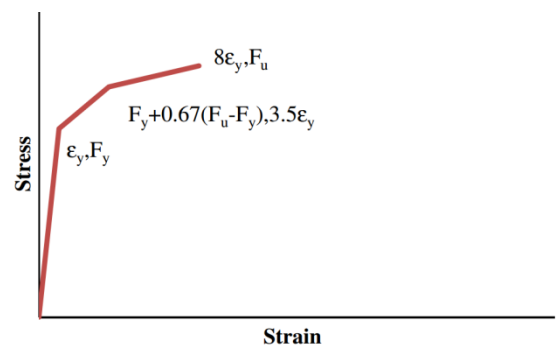


Fig. 13 Stress-strain curve for bolts material

model, mathematical model and experimental results for specimen C1 is shown in Fig. 10. The plot of moment-rotation curves for specimen C2 is shown in Fig. 11. The comparison showed good correlations between the FE model, mathematical model and tested samples, which proved the accuracy in the experimental results.

## 5. Comparison of CPCs and EEPs

To prove the semi-rigid behaviour of CPCs, comparison between EEP (tested in this research) CPCs (tested in previous work) and has been performed by comparing the moment-rotation curves and stiffness of these connections considering that EEP is typical rigid connection (Bai *et al.* 2015, Coelho *et al.* 2004, Scerbo 1996).

### 5.1 Comparison of specimen EEP C1 and CPC C3

Specimen C1 (EEP) and specimen CPC C3 (Nassani, 2014) have the same cross section for the beam and column, dimensions and thickness of the beam and column plates PL1 and PL2, and also same bolt diameter and weld thickness. Fig. 14 shows the plot of moment-rotation curves of EEP C1 and CPC C3.

The initial rotational stiffness can be defined as the slope of moment-rotation curve at initial stage of loading (Kong and Kim 2016, Nassani and Chikho 2015, Salmon *et al.* 2009). In Fig. 14, the initial rotational stiffness of CPC C3 is equal to 10909 kN.m/rad (the slope of the linear part of moment-rotation curve) and for EEP C1 is 14950 kN.m/rad. The ratio of initial rotational stiffness of CPC C3 to EEP C1 is equal to  $10909/14950 = 73\%$ . The reduction in the stiffness is equal to 27%, which proves that CPC C3 has less stiffness comparing with EEP C1.

### 5.2 Comparison of specimen EEP C2 and CPC C4

Specimen C2 (EEP) and specimen CPC C4 (Nassani 2014) have the same cross section for the beam and column, dimensions and thickness of the beam and column plates

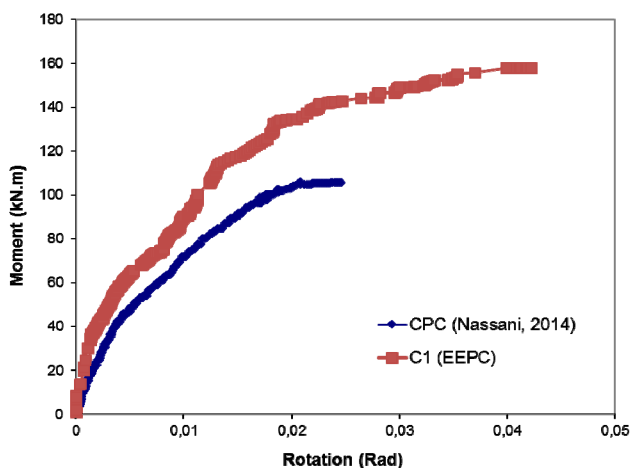


Fig. 14 Comparison between CPC and specimen C1 (EEP)

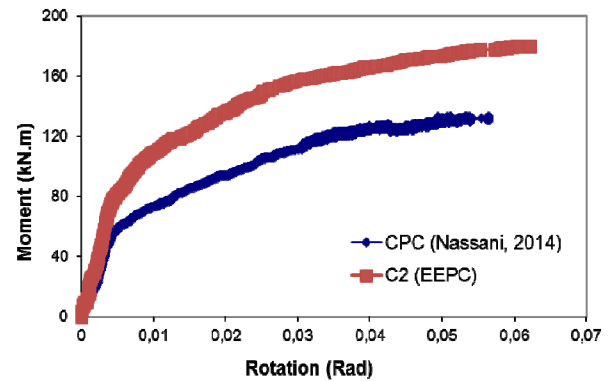


Fig. 15 Comparison between CPC and specimen C2 (EEP)

PL1 and PL2, and also same bolt diameter and weld thickness. Fig. 15 shows the plot of moment-rotation curves of EEP C2 and CPC C4.

The initial rotational stiffness can be defined as the slope of the linear part of moment-rotation curve (Kong and Kim 2016, Nassani and Chikho 2015, Salmon *et al.* 2009). Fig. 15 shows that the initial rotational stiffness of CPC C4 is equal to 11500 kN.m/rad (the slope of the linear part of moment-rotation curve) while it is equal to 15400 kN.m/rad in EEP C2. The ratio of initial rotational stiffness of CPC C4 to EEP C2 is equal to  $11500/15400 = 74.7\%$ . The reduction in the stiffness is equal to 25.3%, which proves that CPC C4 has less stiffness comparing with EEP C2.

## 6. Conclusions

The following conclusions could be drawn from the data developed in the reported study.

- (1) Two full scale of EEPs have been tested and the experimental results obtained enrich the available test data about the behaviour of EEP.
- (2) The power model was used to represent the nonlinear response of EEPs; the power model shows a good agreement with the experimental results, lending confidence in the experimental tests.
- (3) Finite element software ANSYS was used to create and analyze FE models of the specimens. The comparison was based on M- $\theta$  curve of FE models and the corresponding tested samples. The comparison showed good correlations between FE models and the corresponding experimentally tested samples, which proved the accuracy in the experimental results.
- (4) Comparison between moment-rotation curves of EEPs and CPCs has been performed using same beam and column cross-sections; it can be noticed from Figs. 14 and 15 that CPC reduces the stiffness in a range of 25 to 27%.

## References

Abolmaali, A., Kukreti, A., Motahari, A. and Ghassemieh, M. (2009), "Energy dissipation characteristics of semi-rigid

- connections”, *J. Constr. Steel Res.*, **65**(5), 1187-1197.
- AISC ASD (1989), Manual of Steel Construction, Allowable Stress Design; (Ninth Edition), American Institute of Steel Construction, Chicago, IL, USA.
- AISC LRFD (2005), Manual of steel construction, Load and Resistance Factor Design; American Institute of Steel Construction, Chicago, IL, USA.
- Al-Jabri, K.S., Burgess, I.W., Lennon, T. and Plank R.J. (2005), “Moment rotation temperature curves for semi-rigid joints”, *J. Constr. Steel Res.*, **61**(3), 281-303.
- ANSYS Inc. (2013), ANSYS CFX, Release 15.0, USA.
- Bahaari, M.R. and Sherbourne, A.N. (1996), “3D simulation of bolted connections to unstiffened columns – I. T-stub connection”, *J. Constr. Steel Res.*, **40**(2), 169-187.
- Bai, R., Chan, S.L. and Hao, J.P. (2015), “Improved design of extended end-plate connection allowing for prying effects”, *J. Constr. Steel Res.*, **113**, 13-27.
- Baniotopoulo, C.C. and Wald, F. (2000), *The Paramount Role of Joints into the Reliable Response of Structures*, Kluwer Academic Publishers, Netherlands.
- Bose, B. and Hughes, A.F. (1995), “Verifying the performance of standard ductile connections for semi-continuous steel frames”, *Proceedings of the Institution of Civil Engineers, Structures and Buildings*, **110**(4), 441-457.
- Coelho, A.M.G., Bijlaard, F.S.K. and Silva, L.S.D. (2004), “Experimental assessment of the ductility of extended end plate connections”, *Eng. Struct.*, **26**(9), 1185-1206.
- Couchman, G.H. (1997), Design of Semi-Continuous Braced Frames; Steel Construction Institute Publication 183, Silkwood Park, Ascot, Berkshire SL5 7QN, UK.
- Del Savio, A.A., Nethercot, D.A., Vellasco, P.C.G.S., Andrade, S.A.L. and Martha, L.F. (2009), “Generalised component-based model for beam-to-column connections including axial versus moment interaction”, *J. Constr. Steel Res.*, **65**(8), 1876-1895.
- El-Boghdadi, M.H. (1998), “Elastic plastic analysis of semi-rigid industrial frames”, Ph.D. Thesis; KFUPM, KSA.
- EN 1993-1-8:2005 (2005), Eurocode 3: design of steel structures—part 1-8: design of joints; European Committee for Standardization, Brussels, Belgium.
- Faella, C., Piluso, V. and Rizzano, G. (2000), *Structural Steel Semirigid Connections: Theory, Design and Software*, New Directions in Civil Engineering; CRC publishers (EEUU), Boca Raton, FL, USA.
- Fang, C., Yam, M.C.H., Lam, A.C.C. and Xie, L. (2014), “Cyclic performance of extended end-plate connections equipped with shape memory alloy”, *J. Constr. Steel Res.*, **94**, 122-136.
- Hayalioglu, M.S. and Degertekin, S.O. (2005), “Minimum cost design of steel frames with semi-rigid connections and column bases via genetic optimization”, *Comput. Struct.*, **83**(21), 1849-1863.
- Jaspart, J.P., Braham, M. and Cerfontaine, F. (1999), “Strength of joints subjected to combined action of bending moments and axial forces”, *Proceedings of European Conference on Steel Structures-Eurosteel*, Prague, Czech Republic, May, pp. 465-468.
- Jaspart, J.P. and Maquoi, R. (1990), “Guidelines for the design of braced frames with semi-rigid connections”, *J. Constr. Steel Res.*, **16**(4), 319-328.
- Jones, S.W., Kirby, P.A. and Nethercot, D.A. (1983), “The Analysis of Frames with Semi-Rigid Connections-A State of the Art Report”, *J. Constr. Steel Res.*, **3**(2), 2-13.
- Kishi, N. and Chen W.F. (1990), “Moment-rotations of semi-rigid connections with angles”, *J. Struct. Eng., ASCE*, **116**(7), 1813-1834.
- Kong, Z. and Kim, S.E. (2016), “Numerical estimation of the initial stiffness and ultimate moment capacity of single-web angle connections”, *J. Constr. Steel Res.*, **121**, 282-290.
- Lui, E.M. and Chen, W.F. (1987), “Steel frame analysis with flexible joints”, *J. Constr. Steel Res.*, **8**, 161-202.
- Nassani, D.E. (2011), “Static and dynamic behavior of frames with semi-rigid connection”, Ph.D. Thesis; Aleppo University, Syria.
- Nassani, D.E. (2014), “Behaviour of steel cap plate connections: Experimental tests”, *Int. J. Steel Struct.*, **14**(3), 649-657.
- Nassani, D.E. and Chicks, A.H. (2015), “A Simple formula for estimating the column ultimate load with effect of semi-rigid connections”, *Int. J. Steel Struct.*, **15**(1), 31-38.
- Patnana, V. and Vyavahare, A.Y. (2016), “Moment rotation curves for semi rigid connections”, *Proceedings of International Conference on Electrical, Electronics, and Optimization Techniques (ICEEOT)*, Chennai, India, March.
- Penar, B.W. (2005), “Recentring beam-column connections using shape memory alloys”, Master Thesis; School of Civil and Environmental Engineering, Georgia Institute of Technology, Atlanta, GA, USA.
- Salmon, C.G., Johnson, E.J. and Malhas, F.A. (2009), *Steel Structures, Design and Behavior*, (5th Edition), Pearson Prentice Hall, USA.
- Scerbo, J.S. (1996), “Analysis of steel frames with deformable beam to column connections”, M.Sc. Thesis; The University of Manitoba, Canada.
- Tahir, M.M.D., Sulaiman, A. and Saggaff, A. (2008), “Structural behaviour of trapezoidal web profiled steel beam section using partial strength connection”, *Electr. J. Struct. Eng.*, **8**, 55-66.
- Thai, H.T., Uy, B., Kang, W.H. and Hicks, S. (2016), “System reliability evaluation of steel frames with semi-rigid connections”, *J. Constr. Steel Res.*, **121**, 29-39.
- Weynand, K., Jaspart, J.P. and Steenhuis, M. (1998), “Economy studies of steel frames with semi-rigid joints”, *J. Constr. Steel Res.*, **1**(1-3), Paper No. 63.
- Ypma, T.J. (1995), “Historical development of the Newton-Raphson method”, *SIAM Rev.*, **37**(4), 531-555.

BU